Available online at www.CivileJournal.org

Civil Engineering Journal

(E-ISSN: 2476-3055; ISSN: 2676-6957)

Vol. 8, No. 06, June, 2022

Armor Layer Uniformity and Thickness in Stationary Conditions with Steady Uniform Flow

Cahyono Ikhsan [1*], Ariva S. Permana [2], Arlendenovega S. Negara [1]

[1] *Department of Civil Engineering, Faculty of Engineering, Universitas Sebelas Maret, Surakarta, Jawa Tengah, 57126, Indonesia.*

[2] *Department of Civil Engineering, School of Engineering, King Mongkut's Institute of Technology, Ladkrabang, 10520, Thailand.*

Received 11 February 2022; Revised 20 May 2022; Accepted 24 May 2022; Published 01 June 2022

Abstract

The continuous movement of riverbed particles due to turbulent flow determines the stability of non-cohesive riverbeds and banks during riverbed and bank erosion and sedimentation. This study emulated the stable channel design by deriving the low maintenance cost of the channel through bed protection by an armor layer. The study investigated the effects of shear stress and grain size uniformity to determine the minimum non-cohesive armor layer thickness for the stability of riverbeds under steady uniform flow conditions. Experiments were conducted with four different discharges, five armor material gradations, and five bed-slope variations in a full-scale flume. We observed and recorded the behaviors of the five gradations of armor materials for given discharges and bed slopes. Eighty data points were recorded and analyzed. The hydraulic analysis of the flow along with the soil mechanics analysis of the armor materials was done. The soil mechanic analysis was particularly focused on the uniformity coefficient of the armor layer, C_u, to derive the armor layer equation. However, for the manageability of the study, we set the limit of the C_u between 3.0 and 6.0. From the viewpoint of non-erodibility, a wider C_u value indicated a thinner armor layer. Variables that govern the armor layer thickness and the layer thickness itself were derived and proposed. The variables, namely C_u, shear stress (τ_0 and τ_c), and mean diameter of the bed load and armor materials (D_{b50} and D_{a50}). Our results show that these variables governed the thickness of the armor layer, and this is expected to contribute to the design of stable natural channels, which can minimize the cost of irrigation canal maintenance and development.

Keywords: Flow Shear Stress; Armor Layer Thickness and Uniformity; Bed Material Grain Size; Flume; Experiment.

1. Introduction

This study was inspired by the high costs of river maintenance as well as irrigation canal development and maintenance due to erosion and sedimentation. The channel bed and bank erosions have forced us to implement the lined channels, which generated substantial maintenance costs compared to the maintenance-free costs of unlined stable channels [1]. However, in natural conditions, these stable channels were rarely achieved since the channels and rivers were dynamic over time [2, 3]. Therefore, a free or low-cost maintenance channel would be needed. From this background, the study was carried out through the exploration of locally available, free, and abundant armor materials. The results were expected to artificially simulate the stable channels by preventing erosion from occurring. While the challenge was there, there were few studies on the estimation of armor layer thickness under stationary conditions, for example, studies by [4-6] and outdated. This gap has led to the necessity of responding to the challenge we identified through laboratory experiments. The approach of this study was to connect the shear stress on the bed surface, sediment transport rate, and uniformity of the grain size toward the design of the size of the armor layer. Calculating for the

* Corresponding author: cahyonoikhsan@staff.uns.ac.id

http://dx.doi.org/10.28991/CEJ-2022-08-06-01

development of the armor layer is crucial for many reasons since it affects the hydraulic roughness, local availability of bedload, bed permeability, and physical conditions for aquatic organisms [7]. This development can be conducted by introducing locally available and almost cost-free materials, as previously stated, to prevent erosion in the canals via the use of armor layers. Gathering, combining, and assessing existing sediment transport formulas, we performed experiments to understand the phenomena and searched for a simple, yet reliable, armor layer thickness. The experiments led to a simple formula for figuring out the thickness of the armor layer. The diameter of the riverbed sediment, the shear stress, and the armor materials are the variables in the formula.

Continuous movements of non-cohesive riverbed materials induce erosion and sedimentation of river channels, namely riverbeds and their banks, under certain conditions. This continuous movement causes river channel instability due to erosion and deposition of the bed materials. According to Abrahams et al. [8] and Yang and Molinas [9], the total sediment transport, T_s, namely bed and suspended loads, can be expressed in terms of a few governing variables as $T_s = f(\rho, w, Q^{-1})$ in which ρ represents density of water, w indicates the flow width, and Q is the river discharge. Erosion or deposition can be predicted by observing the T_s against the total load under the flow regime in which a predominant flow exists and changes in river morphology in a short period are absent. If the current T_s at a certain section of the river is significantly less than the total load under a flow regime, an erosion process is expected to occur. Theoretically, for non-cohesive riverbeds and banks, the equilibrium state of a natural river can be reached. However, the achievement of such an equilibrium state might be observed for only a short period as the variables that determine the equilibrium change over time. We can distinguish between the equilibrium state of a river, the so-called river regime, and a stable riverbed and banks for non-cohesive riverbeds and bank materials. At equilibrium, the riverbed and banks are normally in a stable condition. One of the indications of a stable condition is the lack of erosion, thus, no sediment transport occurs. In such a case, the bed materials are motionless and remain in their original position despite being under shear stress due to flows. In the same situation, we can also expect that the armor layer grains are motionless and mutually strengthened.

In this study, the armor layer is a type of non-cohesive, naturally shaped material made of gravel of certain sizes that are located on the riverbed in a static position, and the bedload layer is a type of riverbed material that is always actively moving due to river flows. The bedload entrainment develops due to the existing bed shear stress, which is expressed in $\tau = \rho g h s$, and when it exceeds the critical bed shear stress, as $\tau_c = \theta^*(s_g - 1)\rho g d_{50}$ in which ρ represents water density, g is the gravitational acceleration, h = water depth, $S \cong$ slope of riverbed, $\theta^*$is Shields factor, s_g indicates the specific gravity of the river bed material, and d_{50} represents median particle size of the riverbed material. Therefore, when the riverbed materials are subject to shear stress and are not tightly bound, *i.e.*, they are non-cohesive and not protected by the armor layer, the bed materials are eroded, transported, and washed away by the flow. The riverbed sediment would remain in a static state in which its critical shear stress is larger than its bed shear stress. The armor layer structure then protrudes on the riverbed toward the flow, thus blocking the motion of the bedload that passes over it. This process causes an increase in resistance flow, which has an impact on the movement of the bedload into the armor's space. The study was aimed at understanding the behavior of static armor against the flow-generated shear stress for its uniformity, thickness, and erodibility based on results from hydraulic laboratory experiments given various flow discharges under steady uniform flow and a given composition of the riverbed materials. The study limits the focus only on steady and uniform flow, as the existing supporting equipment was unavailable for non-steady non-uniform flow. It was realized that in the real world, the river flows rarely occurred in steady and uniform states. However, we can still argue that at a certain point in a short time, the river flows could be steady and uniform flow. For this reason, the study is still purposeful and useful. Older and more recent relevant studies, which underlie our study, were scrutinized and properly referenced, particularly concerning three issues: (1) layers of the armor, (2) bed shear stress, and (3) uniformity of the armor materials.

1.1. Armor Layers

Bed armoring often develops in a gravel-bed channel with a varied grain size distribution. A streambed could change its grain size composition and particle arrangement due to kinematic sieving, preferential transport, or spontaneous percolation to form various types of surface structures. Zhang et al. [10] show that the bed armoring consists of two processes: surface coarsening and particle clustering. The surface coarsening developed at an earlier stage with low bed shear stress than did the particle clustering at relatively high shear stress. A study by Bettes and Frangipane [5, 11] revealed that a layer of static armor develops when a flow works in a non-uniform riverbed material, and the finest sediment fraction is washed away. This progressive decrease in riverbed materials leaves a fraction of the sediment layer intact and static because of its capability to resist flow-generated shear stress, thus providing sediment input to the flow. Studies concerning static armor with sediment-free input at a uniform and constant discharge have also been done [5, 12]. Proffitt [13] also asserted that the armor layer protects the substratum layer from bed erosion for a given uniformity of armor layer. Parker et al. [14] discussed grain size characteristics in the substrate layer by analysing the amount of sediment transported at a single grain size. Shen and Lu [6] developed a method for predicting the distribution of armor layers. Then, Parker et al. [14] explained the armor layer for each grain fraction and the average diameter of the grains.

Wilcock [15] revealed that the formation of the armor layer must be based on the differences in shear stress that occur in the sand and gravel fractions. Wilcock and Crowe [15] further developed a relationship between the bedload and the armor layer in addition to the substrate, which is reflected in the overall grain size distribution, including the presence of sand grains that fill the gravel during sediment transport.

Curran and Wilcock [16] conducted flume experiments with large discharge intensities and measured the transported bedload and the amount of bedload left at the bottom. The sediment system in the riverbed consists of three layers of forming components, i.e., the surface, substrate, and bedload layers. Parker et al. [14], Wilcock [17], Wilcock and Crowe [15] discussed the surface grain size characteristics. The equation arranged by Parker et al. [9] discussed grain sizes in the substrate. The method proposed by Bakke et al. [18] describes the dependency of armor layer development in surface and substrate layers on the proportions in the mixture of gravel and sand. The combined methods of Wilcock [19] and Bakke et al. [18] were used to measure bottom sediments and the results can be used to calibrate the sediment transport equation. Tan and Curran [20] investigated the formation of armoring clusters. The resulting armor layer structure was a mixture of gravel and sand, which was sorted periodically. Mrokowska and Rowinski [21] stated that the most intensive sediment transport is expected before the discharge peak due to the peak of bedload is most likely around the peak of bed shear stress, provided sediment is available. It seems that the armored bed is destroyed in the region of increased shear velocity. The studies described above support the findings of the current study. The current study was expected to complement an existing study. Based on this premise, our study focused on the effect of shear stress and uniformity of grain size on the thickness of the static armor layer.

1.2. Shear Stress and Transport Rate

Berni et al. [22] found that the equilibrium time associated with a decreased sediment rate in the process of armor layer formation is influenced by four parameters, i.e., the Reynolds number, the non-dimensional median grain diameter, the ratio of the basic shear stress of the channel to the critical shear stress, and the ratio of width to the depth of flow. The research was carried out by collecting laboratory data to study the sediment transport rates without an upstream sediment supply under steady-flow conditions. Wilcock and Crowe [15] found that the content of sand strongly influences the rate of coarse grain/gravel transport and the total sediment transport rate. In mixed conditions of sand and gravel, the increase in the rate of coarse grain transport will grow rapidly with sand contents in the range of 15% to 27%. The grain sizes of the riverbed materials varied with the sand content. However, the results of laboratory experiments demonstrate that minimal or no effects of the surface roughening process occurred with changes in the flow rate and the rate of transport of the grain material. Wilcock [19] developed empirical, but practical methods, to estimate the amount of gravel and sand transported separately, knowing only the shear stress of gravel or sand riverbed. This estimation is important, particularly because of its practical applications for predicting the movement of riverbed materials, given the limited available information.

In addition to sediment transport models of separation of sand and gravel riverbed materials, Wilcock and Crowe [15] presented a transport model for mixed sand/gravel sediments. This model uses the full-size distribution of the layers, including sand, and incorporates the nonlinear effect of sand content on gravel transport rates that were not included in the previous model. Sediments with fine material or sand tend to form a relatively coarse median grain size of riverbed materials. The sediment supply regime provides first-order control on bedload transport rates, which are significantly influenced by mobile sediment over the flow and bed surface texture [23]. It shows evidence that cycles of degradation and aggradation occurred due to sediment feed upstream, bed composition, bed topography, and the rate and texture of sediment output. Transport rates of bedload usually show wide fluctuations, even under steady flow conditions. The group variance of transport rate is controlled simply by the sampling duration and its mean rate [24].

1.3. Coefficient of Uniformity (C_u)

The coefficient of uniformity of the sediment samples is one of the significant parameters in determining the armor layer. According to the sediment classification criteria of the Unified Soil Classification System (USCS), the coefficient of uniformity indicates a range of sediment grain diameter sizes that can be obtained from the grain-size curve. If the C_u value is large, the grain size range is wide. The width of C_u shows that the grain sizes of the sediment vary, and therefore, how well it is well graded. However, if the C_u value is small or quantitatively the value of C_u is less than 4, the grain size is more uniform and poorly graded. Based on USCS, the uniformity coefficient is in which D_{60} indicates a designated diameter in which 60% of the sample passed the gradation analysis. Similarly, D_{10} means 10% of the sample or finer material passed a specific diameter in the gradation analysis. The C_u with the ratio of D_{60} and D_{10} is normally used as a gradation of embankment material. Therefore, it is not suitable for the armor layer, which is continuously under shear stress. Limerinos [25] proposed a modified C_u for the river bed materials resulting from experiments on bed roughness with natural materials or river bed materials. The Cu could be defined as $C_u = D_{84}/D_{16}$.

In our experiments, the range of the C_u value decreased and therefore, the bed roughness became larger, which resulted in a steeper bed slope for the same flow rate. Based on USCS criteria, Limerinos [25], other studies, and physical observations from our laboratory, we proposed a C_u value $C_u=D_{84}/D_{16}$. For the river bed materials, a narrow range of C_u is preferred, indicating the diameters of upper and lower limits are close to one another, and the riverbed materials are approximately uniform. Based on this condition, the thickness of the armor layer would be smaller. However, since this finding was uncertain, it was decided to do experiments using seven C_u values with a range from 3.0 to 6.0.

1.4. Measuring System and Accuracy

During the experiment, we measured all variables i.e. hydraulics and sediment materials by using a metric system. The accuracy applied for the measurements depends on the object measured, for example, for the size of sediments, armor layer, and hydraulic variables we used one significant figure with the accuracy of 0.1 mm. For the water depth, the accuracy was 0.1 cm. The flow discharge also adopts one significant figure with the accuracy of 0.1 liters per second (l/s) during the flow discharge calibration process. However, for the calculation, two digits of accuracy for all variables were adopted.

2. Methodology

2.1. Experimental Arrangement

We carried out the experiments on a full-scale hydraulic model of the flume, armor size as well as hydraulic parameters of Reynolds Number and Froude Number, and therefore, there were no scale effects of model-prototype on the results of the experiments. The experiments were conducted in a hydraulics laboratory using a plexiglass sediment recirculating flume 0.60 m wide, 10 m long, and 0.45 m high. The method of the experiment is schematically shown in Figure 1.

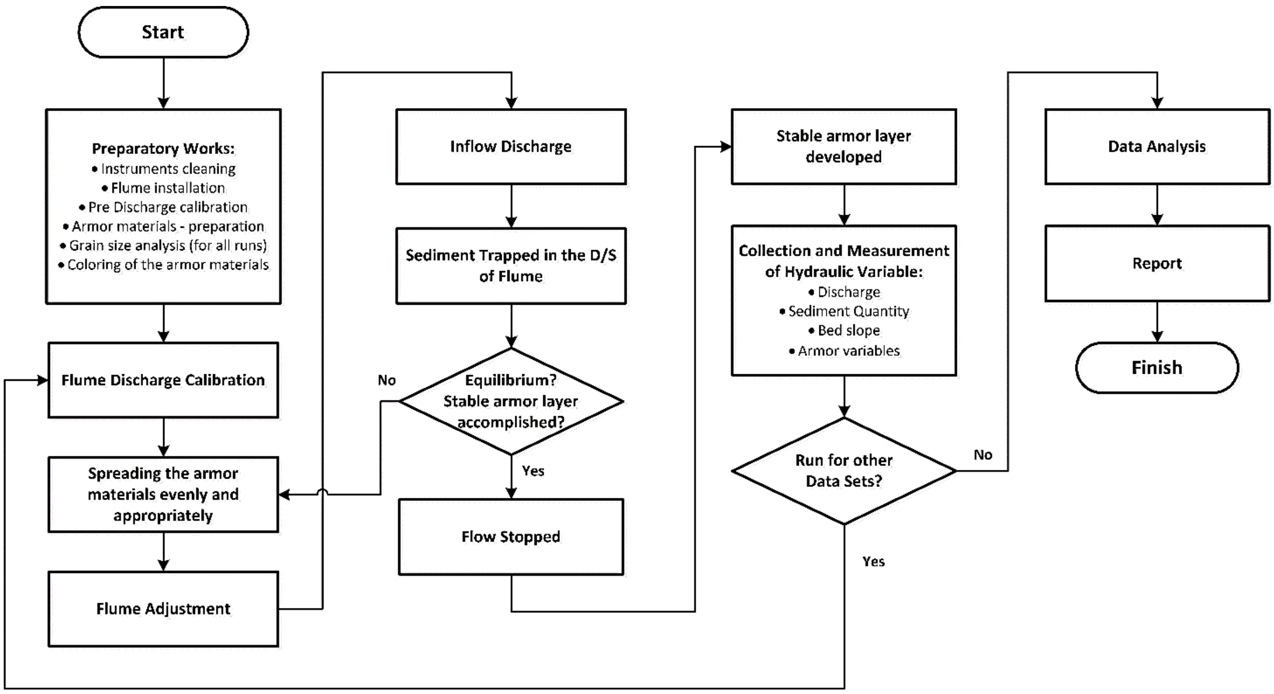

Figure 1. Flowchart of the Method of Experiment

The flume was specifically designed to examine various sediment transport phenomena with variations of the bed slope, as depicted in Figure 2.

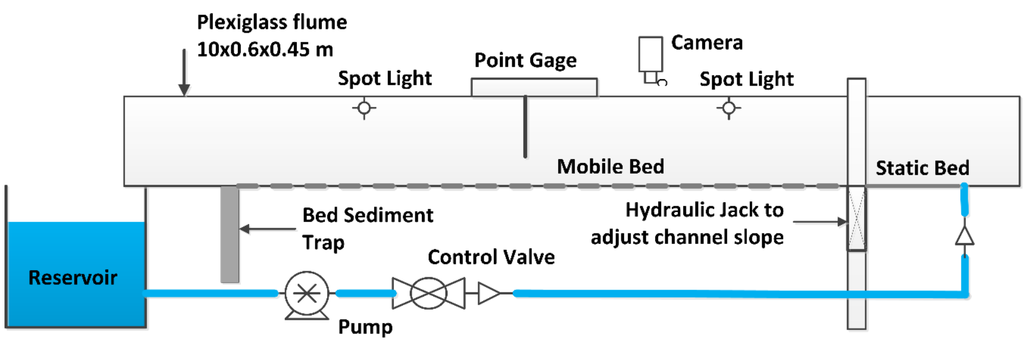

Figure 2. The flume setup

The experiment employed a full-scale flume and used a digital point gauge (Figure 3-a), current meter (Figure 3-b), and sediment traps (Figure 3-c). The flow speed was measured by using the current meter at the middle position of the flume and above the base surface at 0.20h, 0.50h, and 0.85h, where h is the depth of flow. The velocity was averaged from the velocities of flows at these depths, and consecutively the discharge was calculated.

(a) (b) (c)

Figure 3. (a) Point gauge for channel bed elevation measurements, (b) velocity measurements, (c) sediments trap

The experiment was run with four different discharges of steady uniform flow, five groups of material gradations, and five bed-slope variations. Therefore, the total number of runs was 100. The bed slopes of the channel in this study were 1.0%, 1.4%, 1.8%, 2.2%, and 2.6%. The bed slope variations were controlled by adjusting a regulator that was attached to a hydraulic jack in the experimental apparatus. Discharge variations of 25, 30, 40, and 45 L/s were adopted for the flow rates in the flume. Our experiments were bound by the discharge capacity of the flume for which the maximum value was about 70 L/s. We could, therefore, in practice, only run the experiments with discharges between 10 and 60 L/s. By this limitation, the experiment was conducted with the initial discharge set at 20 L/s in the hope that this rate would generate an incipient discharge. However, with the initial discharge of Q = 20 L/s, the average depth of water in the flume was only 5–6 cm, which generated maximum shear stress, $\tau_o = 9.5\ N/m^2$, which was small. Concurrently, the critical shear stress of the sediment was 15 N/m^2. The initial discharge of 20 L/s did not generate bed sediment motion and was not considered an incipient discharge was not used. The discharge was then increased using an arbitrary incremental discrete value of 5 to 10 L/s. With a 5 L/s incremental discharge, the initial discharge was increased to 25 L/s. The theoretical incipient discharge was computed by assuming the initial motion of the bed sediment by equalizing the critical shear stress of the bed sediment and the shear stress generated by flow. Then, the incipient discharge was calculated. The incipient discharge was computed using the following series of equations.

The critical depth that generates the motion of the sediment is computed using the Equation 1:

$$h = \frac{\theta^*(S_g - 1)d_{50}}{S} \tag{1}$$

The incipient discharge was estimated using the Manning formula, provided that the flow depth is given by the Equation 2:

$$Q_1 = \frac{bh}{n} R^{0.67} S^{0.5} \tag{2}$$

From Equations 1 and 2 for a rectangular channel width of b = 0.6 m, S = 0.02, and n = 0.008, specific gravity of the sediment S_g = 1.65, and d_{50} = 3.0 mm, the incipient discharge rate was found to be 21 L/s. At this discharge rate, the bed sediment began to move. Based on this incipient discharge, the initial discharge of the experiment was taken to be 25 L/s with increment discharge of 5 to 10 L/s. The discharge rates in the experiment were 25, 30, 40, and 45 L/s.

The riverbed materials for the armor layer were grouped into five categories based on their mean diameter (D50), with mean diameter (D50) of (1) M1 of 90 mm, (2) M2 (D50 = 23 mm), (3) M3 (D50 = 42 mm), (4) M4 (D50 = 15 mm), and (5) M5 (D50 = 59 mm). The gradation of the M1 to M5 materials is shown in Figure 4. For the armor itself, each piece of gravel of the same size group was represented by different color to observe the hydraulic behavior of the individual gravel groups.

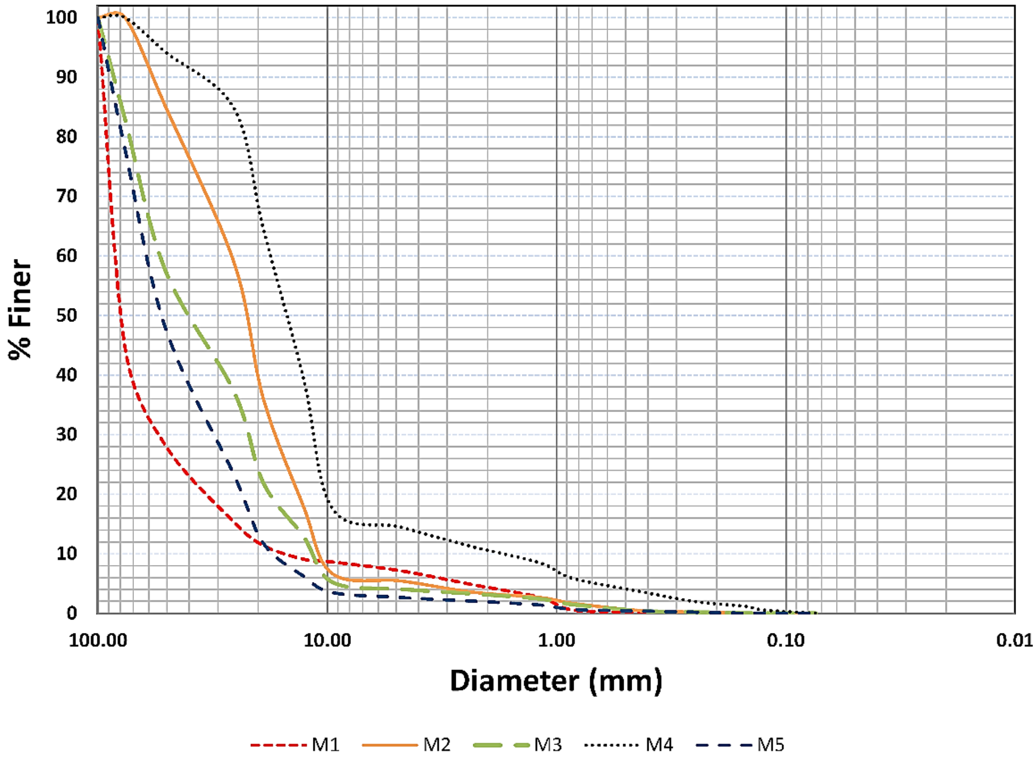

Figure 4. Gradation of Five River Bed Materials (M1-M5)

2.2. Measurements of Variables

For every experiment, for each group of material, gravel and sand were mixed and then evenly distributed along the channel at a thickness of 15 cm, while at the downstream end of the channel a sediment trap box was installed to catch the flushed materials. Furthermore, the slope of the channel was adjusted and the flow rate was set. Observations of flow conditions were conducted until steady uniform flow conditions were achieved. Measurements and observations of water level elevations in each experiment were carried out as controls for the bottom slope of the sediment.

In each run, the behavior and variables were recorded when steady uniform flow conditions were achieved, at this time, the flow depths were the same at any position along the flume. The measurements at every run included the flow velocity, water temperature, water level profile, and amount of transported bottom sediment. Measurement of flow velocity was done by installing a current meter in the middle of the flume at three vertical locations, namely 0.2, 0.4, and 0.8 of water depth (h), after which the depth of flow and captured sediments were measured accordingly. The sediments accumulated in the sediment traps were collected at 2 min intervals, weighed, and recorded. Sediment traps are tools used to catch sand that moves out *via* the downstream channel. The run for each dataset continued until the sediment captured in the sediment traps was 0% of the transported sediment. At the final stage of each run, sediment was taken from the flume and a sieve analysis was performed to yield a grain gradation profile of armor, substrate, and bedload layers.

3. Results and Discussion

3.1. Shear Stress

We run the experiment with four data sets of discharges (Q1 to Q4), four data sets of bed slope (S1 to S4), and five data sets of materials (M1 to M5). We have, therefore, 80 sets of results. For these 80 sets of results we computed the Froude number (Fr), and bed shear stress (τ). We also measured the flow velocity (U), and flow depth (h). Each data sets for the experiment is denoted by $M_iQ_jS_k$ where i = 1 to 5, j = 1 to 4, and k = 1 to 4. Table 1 shows an example of the running combinations of material groups, namely the M1, with four (4) discharge data sets (Q1–4) and five (5) different bed slopes (S1–5) with corresponding shear stress τ_o. For all flow rates, it was found that the experiments were under steady uniform (Q is constant), and flow is sub-critical ($Fr < 1.0$).

Table 1. Measured and computed variables for M1, Q1–4, and S1–5 data sets

Running	Discharge *Q* (l/s)	Bed slope *S*	Flow velocity *U* (m/s)	Flow depth *h* (m)	Froude Number F_r	Shear stress τ_o (N/m^2)
M1Q1S1	25	0.010	0.529	0.080	0.597	7.830
M1Q1S2	25	0.014	0.604	0.070	0.705	9.610
M1Q1S3	25	0.018	0.660	0.065	0.797	11.478
M1Q1S4	25	0.022	0.701	0.060	0.878	12.949
M1Q1S5	25	0.026	0.729	0.055	0.951	14.028
M1Q2S1	30	0.010	0.562	0.090	0.598	12.500
M1Q2S2	30	0.014	0.626	0.080	0.706	13.000
M1Q2S3	30	0.018	0.685	0.075	0.799	13.244
M1Q2S4	30	0.022	0.730	0.070	0.881	15.107
M1Q2S5	30	0.026	0.762	0.065	0.955	16.579
M1Q3S1	40	0.010	0.621	0.110	0.598	13.800
M1Q3S2	40	0.014	0.701	0.100	0.708	14.700
M1Q3S3	40	0.018	0.754	0.090	0.802	15.892
M1Q3S4	40	0.022	0.809	0.085	0.886	18.345
M1Q3S5	40	0.026	0.852	0.080	0.962	20.405
M1Q4S1	45	0.010	0.648	0.120	0.597	14.300
M1Q4S2	45	0.014	0.735	0.110	0.708	15.107
M1Q4S3	45	0.018	0.795	0.100	0.803	17.658
M1Q4S4	45	0.022	0.834	0.090	0.887	19.424
M1Q4S5	45	0.026	0.906	0.085	0.964	21.680

The runs of the other four riverbed material groups (M2–M5) were carried out similarly, but the outputs are not presented here. From these 80 datasets we observed in our experiments, 20 datasets are presented. They resulted from corresponding sediment discharges, Q_s, as shown in Figure 3. Regression lines were also produced to obtain the critical shear stress, which is the intercept of τ_o when the sediment discharge, Q_s was equal to zero.

From Figure 5, it can be observed that the critical shear stress for Group 1 riverbed material (M1) under four discharge variations (Q1 to Q4) and five different bed slopes (S1 to S5) converge towards the value of ≅ 3.0 N/m^2. Equalizing the critical shear stress, τ_c, of Shields [26] and the reference bed shear stress, τ_0, resulted in the minimum gravel bed diameter shown in Equation 3 for the armor layer. This process is summarized in Table 2.

$$d_s = \frac{\tau_c}{\rho g (s-1)} \tag{3}$$

Table 2. Critical shear stress (τ_c) and corresponding d_s for the group of M1 Q(1-4), S(1-5)

Group	Equation	Critical Shear Stress, τ_c N/m^2	Sediment diameter, d_s mm
M1Q1S(1-5)	$\tau_o = -0.0002Q_s^2 + 0.0954Q_s + 3.022$	3.022	0.118
M1Q2S(1-5)	$\tau_o = -0.0002Q_s^2 + 0.1069Q_s + 3.051$	3.051	0.119
M1Q3S(1-5)	$\tau_o = -0.0002Q_s^2 + 0.1096Q_s + 3.018$	3.018	0.118
M1Q4S(1-5)	$\tau_o = -0.0002Q_s^2 + 0.1122Q_s + 3.039$	3.039	0.119

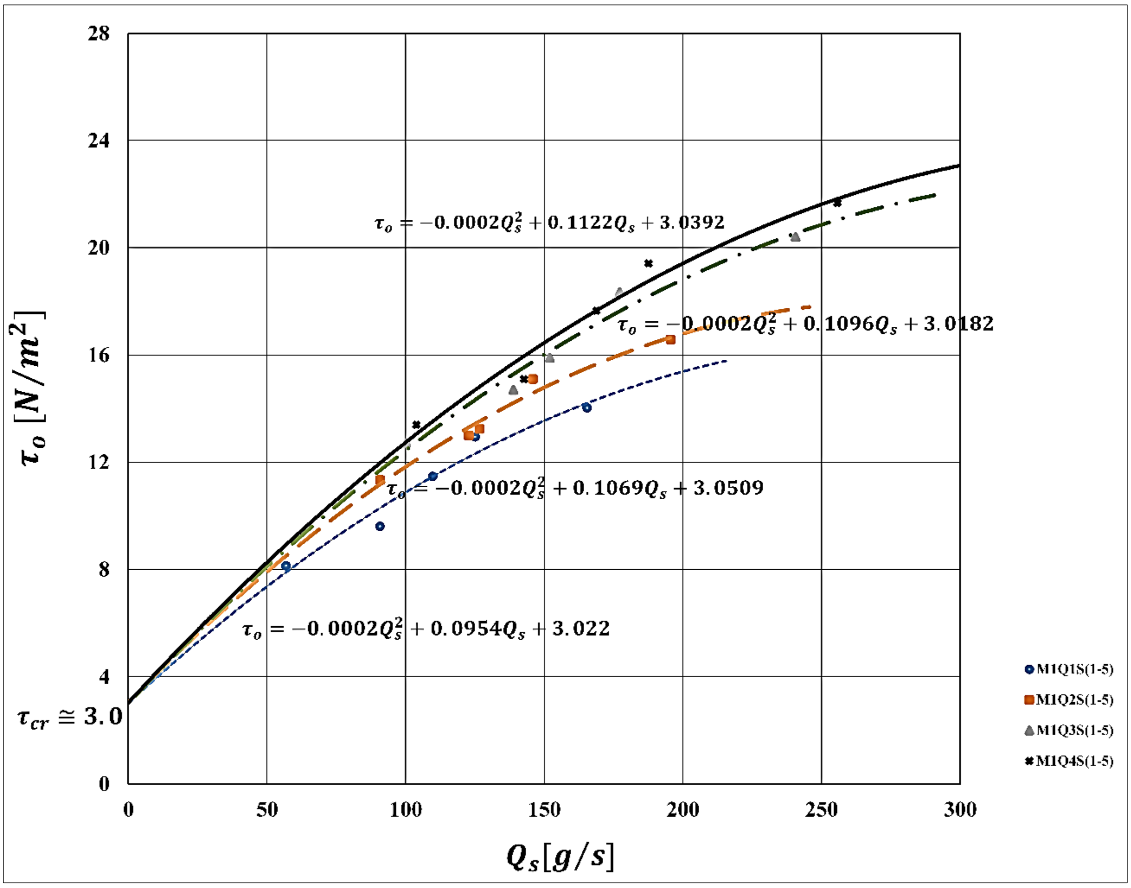

Figure 5. A correlation between bed shear stress and bedload transport

From Table 2 and also exhibited in Figure 5, for group 1 (M1) of armor materials, for all groups of inflow discharges (Q1 to Q4), and all groups of riverbed slopes (S1 to S5), the critical shear stresses at the river bed, where no bed materials were transported ($Q_s = 0$) were between 3.018 and 3.051 N/m^2, these values correspond to the minimum sediment diameter of 0.118 mm. With this minimum diameter of bed material, the river bed erosion would not take place. Thus, the minimum diameter of armor is theoretically around this size. For practicality, an armor layer could be designed with the minimum diameter of that size where the tractive force generated by flow is less than the critical shear stress of the armor layer. The armor materials could be originated from any locally available sands or gravel quarry and should undergo gradation analysis by setting the minimum diameter. The thickness of the armor layer could be determined by considering other factors.

3.2. Bed Load Sediment Transport

Bedload transport plays an important role in shaping the longitudinal profile of a stream channel [24]. Bedload sediment transport is a certain structure of sediment transport, which involves sand, gravel, or coarser particles saltating or rolling along the streambed [24]. The reasons why bedload transports difficult to predict: the mix of fast and slow processes, non-equilibrium and noise-driven processes, the varying temporal and spatial scales dependent on flow conditions, the heterogeneity of materials and flow conditions, nonlinearity, threshold effects, poor knowledge of initial and boundary conditions, and scale effects between laboratory and field conditions [24]. Bedload transport rates are completely parameterized concerning the size of the bedload. That is, rather than specifying a size distribution for each rate, reliance is placed on a representative particle size derived from an aggregated sample of the bedload, or an extrapolation that is dependent upon the size distribution of a textural facies in the local bed material [27]. Our experiments demonstrate two phases of sediment transport, namely, riverbed erosion followed by an equilibrium phase during which no further erosion occurred. The riverbed erosion phase was the initial phase characterized by the movement of the bed load grains from the bottom until either of two conditions were satisfied: (1) the maximum value of transported bottom grain was achieved or (2) the present shear stress did not exceed the critical shear stress of the remaining riverbed sediment. The equilibrium phase was the final phase. It shows a gradual decrease in the movement of the transported riverbed grains. Therefore, a stable riverbed surface was created. In the experiments, if this condition was achieved, the flow was then stopped. It appears that the grains left on the bottom surface consisted of gravel and various sand types. However, the amount of gravel was more predominant with grains arranged in a relatively uniform cluster, as depicted in Figure 6.

Figure 6. The final results of each run of the data set in the experiment yielded a protective coating on the channel bed

The armor layer had a grain gradation that tended to be homogeneous in size with an average diameter that was larger than the substrate layer. The presence of bed grains in the space of the armor layer began with gravel blocking the movement of the bed grains that passed above it. Therefore, those grains entered gravel cavities and remained under shelter in such locations. An exchange between the bed grains in the cavity results in interlocking action. Small diameter grains were not observed. According to an identical experiment conducted by Wang et al. [28], some clusters structures and linear structure was developed after the complete coarsening of the bed. Those bed conditions would significantly increase the stability of the bed, provide a large impact on the bed load transport, and change bed composition [29]

The process of transporting sediment is the displacement of granular sedimentary material by the flow of water in a river section. Transport occurs in the direction of the flow so that it can be seen whether or not under certain conditions equilibrium, erosion, and deposition conditions would exist. When the sediment transport is under a state of erosion and deposition, bed sediment movement occurs in rolling, sliding, and jumping actions. Figure 7 shows the weight of sediment measured at 2 min intervals for a run of one data set, the M1Q1S1 experiment. The flow is stopped when sediment is no longer transported by the flow.

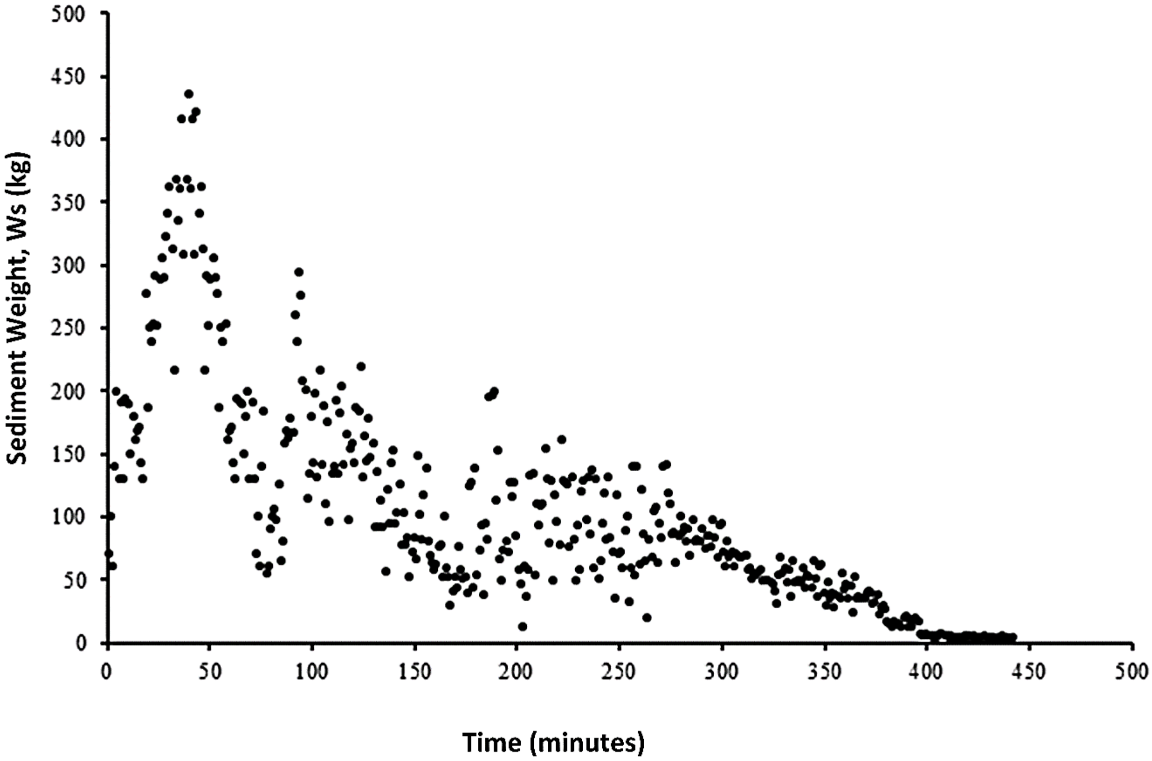

Figure 7. Weight of transported sediment

As shown in Figure 7, the maximum quantity of sediment transported occurred in the 42nd min for 0.448 kg, while no more sediment was transported after 390 min. It could be explained that after 42 min, the layer of sediment materials was interlocked in such a way that the existing shear stress did not exceed the critical shear stress of the remaining sediment layer. In this case, the armoring process began. Figure 7 shows an identical result to the experiment conducted by Wang et al. [29] that the formation and reestablishment of the bed load transport rate in the static armor layer increased from zero to its peak before decaying.

This result is also similar to that of Proffitt [13] concerning the formation of an armor layer on a channel bed. The channel bed material used in this experiment was a non-uniform material under constant sub-critical steady uniform flow conditions. The duration of the experiment was between 24 and 90 h. The process of forming the armor layer, in general, is related to the movement of the bottom sediment in which the amount of sediment transported in the first hour reaches its maximum, which can be as much as 50% of the total transported sediment. Our experiment also presents results similar to those of Henderson [30] in which the formation of an armor layer on a channel surface occurred rapidly. This formation was indicated by the presence of transported sediments that had reached the maximum amount.

The sediment left on the bottom consisted mainly of gravel-type materials with larger diameter grains with cavity formation between the constituent grains. The structure of the layer always prevented the movement of the grains that passed over it. At this stage, a large sediment size was quite visible on the bottom surface. The position of the long axis of sediment grains was arranged in a position perpendicular to the flow direction, thus forming a network. This condition had a positive effect on the formation of a surface protective layer. Other observations showed that the position of the sediment grains was more stable. They did not move and were able to protect the surrounding grains. The movement of the grains above the riverbed layer by rolling, sliding, and jumping was determined by the shape of the grains, but some would remain and occupy positions between the cavities of the protective layer structure while the rest would continue to move until they found the right position among the larger grain cavities. Streambed topography adjusts to the reduction in sediment supply not only through surface coarsening but also through a decrease in change of bed surface cluster and streambed mobility [7].

3.3. The Thickness of the Static Armor Layer: The Main Finding of the Study

To accomplish the objectives of this study, we observed that the mean grain diameter of the armor layer (D_{a50}), the mean grain diameter of the bed layer (D_{b50}), bed shear stress (τ_o), critical shear stress (τ_c), and grain size uniformity (C_u). Based on previous studies and our observations during the experiments, the primary governing variables that influence the armor layer thickness are τ_o and C_u. If $C_u = 1$, the armor layer gradation was uniform, and the minimum grain size diameter of the armor could be approximated by Equation 3, and the thickness (t_a) could be practically taken as 3 to 5 times that of the armor diameter. However, if $C_u > 1$, the thickness of the armor layer must follow the governing variables. The parameter, t_a, is expressed as a function of some governing variables as shown in Equation 4.

$$t_a = f(D_a50, D_b50, C_u, \tau) \tag{4}$$

The variables can be expressed in dimensionless for as shown by Equation 5:

$$f' = \left(\frac{t_a}{D_{a50}}, \frac{D_{a50}}{D_{b50}}, \frac{\tau_0}{\tau_c}, C_u\right) \tag{5}$$

From Equation 5, it is seen that all components of f' were positive and could be expressed as showing a correlation between the armor layer thickness and the remaining parameters, as shown by Equation 6:

$$t_a = K\left(\frac{D_{a50}}{D_{b50}}\right)\left(\frac{\tau_0}{\tau_c}\right) C_u D_{a50} \tag{6}$$

A coefficient K was introduced for the safety of the armor layer in addition to minimizing the cost of the materials in a permanent artificial lined channel, such as concrete, masonry, and others. In our experiments, we found that the optimal K values were between 1.5 and 2.5. Equation 6 yielded a reliable armor layer thickness for the bed protection of our common natural rivers. If the mean diameter of bed load sediment was smaller than the mean diameter of the armor material, it presented a thicker armor layer. This is sensible as the protected grain size was smaller at smaller critical shear stress, τ_c, against the existing shear stress, τ_o. The ratio between shear stress generated by flow and critical shear stress of the armor was also reasonable as the armor must be resistant to the shear stress, τ_o. The uniformity coefficient of the armor materials, C_u, can be used to directly determine the thickness of the armor layer. An ideal armor layer occurs when C_u is close to 1.0 or the armor materials are uniform. Thus, a larger C_u the value indicates more heterogenous grain sizes of the armor materials and yields a thicker armor layer. This situation is realistic and practical. Another practical aspect of Equation 6 is its simplicity and capability to adjust to local conditions after the introduction of a K coefficient. Equations 4 and 5 that lead to the derivation of the thickness of the armor layer can be considered the primary findings of the study.

Twenty random data points were selected in our samples with single discharge to corroborate the plausibility and reliability of Equation 6, as shown in Table 3.

Table 3. The armor layer thickness, which is based on random data points in the study for Equation 6

Armor Mean Diameter, D_{a50} in mm	Mean Diameter of Riverbed Sediment, D_{b50} in mm	Shear Stress (generated by Flow), τ_o in N/m^2	Critical Shear Stress of the Riverbed sediment, τ_c in N/m^2	Coefficient of the Uniformity of the armor material, C_u (Dimensionless)	Armor Thickness, t_a in mm
51.0	2.4	16.18	15.49	4.71	103.2
54.0	2.3	16.18	14.96	4.50	111.9
56.7	2.3	16.18	14.75	4.32	116.0
59.7	2.3	16.18	14.63	4.37	125.6
62.3	2.3	16.18	14.45	4.15	127.8
56.2	2.5	16.18	16.01	4.05	91.6
56.8	2.4	16.18	15.53	3.86	93.7
61.9	2.4	16.18	15.35	3.73	101.0
69.5	2.4	16.18	15.25	3.61	111.2
69.5	2.2	16.18	13.89	3.23	120.0
59.8	2.6	16.18	16.53	3.61	81.4
63.8	2.5	16.18	16.14	3.46	87.4
66.0	2.2	16.18	14.23	3.36	112.9
67.5	2.0	16.18	12.54	3.27	144.9
69.9	2.01	16.18	12.82	3.07	134.8
65.3	2.61	16.18	16.66	3.27	79.4
68.2	2.56	16.18	16.30	3.27	86.5
70.0	2.27	16.18	14.49	3.19	109.7
71.8	2.16	16.18	13.74	3.22	126.5
74.3	2.17	16.18	13.87	3.14	125.3

The safety factor against bed erosion, K = 1, yielded a reasonable thickness of the armor of 80 to 140 mm for an average diameter of the armor of 50 to 70 mm. The K coefficient can vary depending on local conditions.

To ascertain the uniformity of designed armor materials, we examined the average of the coefficient of uniformity, which was determined as $C_u = D_{90}/D_{16}$. Its standard deviation shows an average value of C_u, 3.5, with a standard deviation of 0.7, and a range of 2.9 (with the maximum and minimum values of 5.3 and 2.4, respectively). The armor materials used in the experiment varied with a relatively narrow standard deviation. With 80 data points, it is safe to say that the designed armor materials are sufficient to support the results.

The exact comparison of the armor layer thickness could not be carried out since we could not find the references for river bed protection. While the works of Griffith [1], Curran and Wilcock [16], and Wilcock & DeTemple [17] that we referred, to have indeed given some insights on the armor layer for riverbed protection including the estimate of armor size, and in such a case we have a similar approach to the armor size, which is bed shear stress generated by flow, on the other hand, they did not provide an explicit estimation on the thickness of the armor layer. There were some studies on armor for example [31, 32], but the studies were largely for the armor of the breakwater. However, a study by Escarameia (1999) [33] given an estimate of armor layer thickness as shown in the Equation 7:

$$D_n = \frac{0.037\, U^2}{(S_g - 1)} \tag{7}$$

where, D_n is armor layer thickness, U is average flow velocity, and S_g is specific gravity of the armor material. It seems that the derivation of Equation 7 was largely based on the empirical method, even though the primary approach was the same, which is bed shear stress.

The implication of this finding is mainly in the way we view the design of stable channels: (1) the hydraulically stable channels are seen not only from the perspective of the absence of erosion in the channel but also from no sedimentation. This situation needs a balance between no-erosion and no-sedimentation states. The no-erosion state can be simply achieved by controlling the permissible flow velocity, but too small a flow velocity may lead to the sedimentation process in the channel. These two situations are undesirable, and certainly difficult to accomplish as it is theoretically a point rather than a range of values, as illustrated in Figure 8 (2) we may need our irrigation channels to be hydraulically stable, as we wish to minimize the maintenance costs. We design the channel by using the principles of the design of a stable channel. However, we cannot always accomplish it, since many factors contribute and some of them are beyond our control (3) If a hydraulically stable channel could not be accomplished because of the uncontrollable factors, we should look into any possible solutions, such as armor layers, revetments, ripraps and the likes (3) the armor layers as proposed by this study can be developed by utilizing locally available sands and gravels.

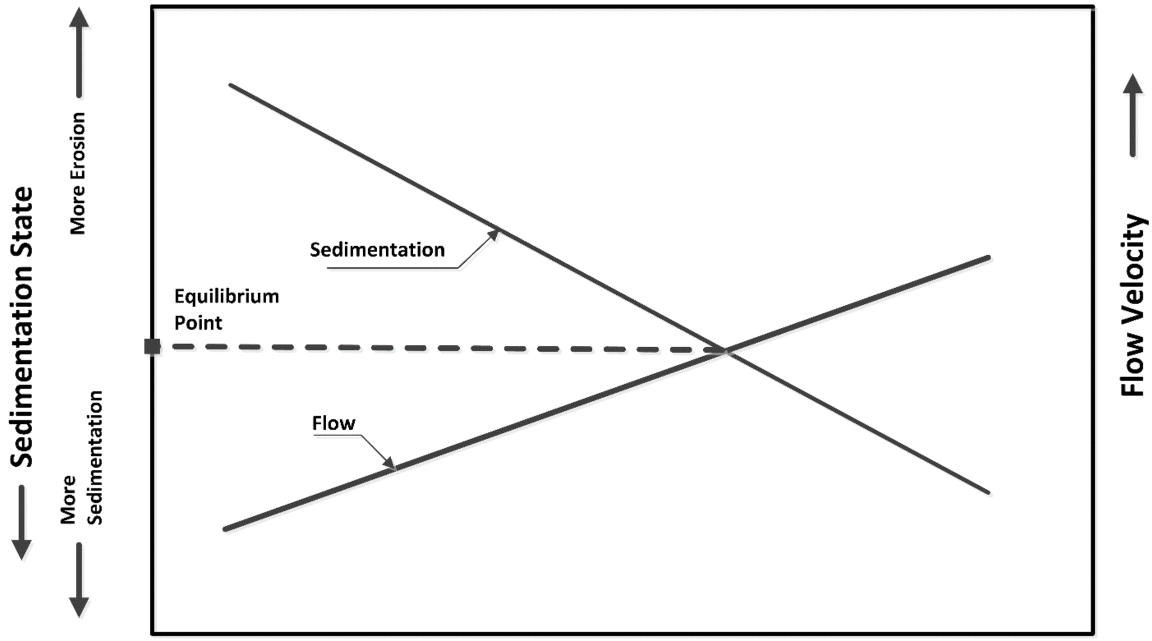

Figure 8. Two States in Design Stable Channel

As an epilog to this study, the practical equation for determining the armor layer thickness may hopefully contribute to theoretical and practical practice, particularly in the sediment transport field and to river engineering in general.

4. Conclusions

Our experimental study was initially inspired by the high costs of irrigation canal maintenance as well as flood control channel development and maintenance due to erosion and sedimentation in the canals. It attempts to reduce such costs to an affordable level. This development can be done by introducing locally available and almost cost-free materials to prevent erosion in the canals via the use of armor layers. Gathering, combining, and assessing existing sediment transport formulas, we performed experiments to understand the phenomena and searched for a simple, yet reliable, armor layer thickness. The key findings of this study are (1) the development of a formula for designing the thickness of the armor layer in which the variables are riverbed sediment diameter, shear stress, and armor materials. This formula is represented in Equation 6. (2) During the experiment, we confirmed the role of riverbed shear stress in the sediment transport phenomena, as the sediment transport formula requires only a few variables. (3) Based on the observations of the bed material's behavior, we assert that the approach of stable channel design principles should not be based only on a non-erosion state but also on a non-sedimentation state. While we assert that both states must be taken into account, as the hydraulically stable channel implies non-erosion and non-sedimentation states, the conventional theory of design of stable channels should be revisited.

The conventional principles of the design of stable channels were fundamentally founded on several parameters: (a) the channel regime theory, which is based on the empirical concept in which the equilibrium state of the river’s hydraulic variables has certain correlations; (b) the tractive force methods, which consider bed erosion due to the flow-generated tractive force exceeding the critical shear stress of river bed materials; and (c) the sediment transport optimization principle, which assumes quasi-equal quantities of sediment along the river for a certain uniform discharge (see studies by Bettes and Frangipane [11]; Eaton and Millar [34], and Ackers and White [35]. However, we should take note of the limitations of the study, in which the experiment was basically based on steady and uniform flow, and therefore other effects might not be taken into account. This limitation might be a challenge and an arena for future research, and thus possible unanswered questions can be addressed. Our findings also show a consistent result with the current theory of sediment transport optimization as exhibited by [8, 22, 36], and the results show that riverbed erosion could be prevented by protecting the bed materials from flow-generated shear stress. It is tantamount to a lined channel but with the provision of locally available and low-cost armor materials that would correct shear stress-induced damage and become material groups for the armor. Our study combined the tractive force method with the sediment transport optimization principle. Since the principles of this study are in line with the design of stable channels, it is safe to say that the study's results could add to and improve current theory and practice in designing stable channels.

5. Declarations

5.1. Author Contributions

Preliminary idea, C.I.; conceptualization, C.I. and A.S.P.; methodology, C.I., and A.S.N.; formal analysis, C.I., A.S.P., and A.S.N.; writing—original draft preparation, C.I., A.S.N., and A.S.P.; writing—review and editing, A.S.P.; visualization, C.I., and A.S.P.; supervision and project administration, C.I.; funding, C.I. All authors have read and agreed to the published version of the manuscript.

5.2. Data Availability Statement

The data presented in this study are available on request from the corresponding author.

5.3. Funding

The authors received no financial support for the research, authorship, and/or publication of this article.

5.4. Conflicts of Interest

The authors declare no conflict of interest.

6. References

[1] Griffiths, G. A. (1981). Stable-channel design in gravel-bed Rivers. Journal of Hydrology, 52(3-4), 291–305. doi:10.1016/0022-1694(81)90176-1.

[2] Everard, M., & Powell, A. (2002). Rivers as living systems. Aquatic Conservation: Marine and Freshwater Ecosystems, 12(4), 329–337. doi:10.1002/aqc.533.

[3] Iberall, A.S. (1987). On Rivers. Self-Organizing Systems. Life Science Monographs. Springer, Boston, United States. doi:10.1007/978-1-4613-0883-6_3.

[4] Ettema, R. (1984). Sampling armor-layer sediments. Journal of Hydraulic Engineering, 110(7), 992-996. doi:10.1061/(ASCE)0733-9429(1984)110:7(992).

[5] Lamberti, A., & Paris, E. (1992). Analysis of armouring process through laboratory experiments. Dynamics of gravel-bed rivers, John Wiley & Sons, Chapter 11, 227-250.

[6] Shen, H. W., & Lu, J. Y. (1983). Development and prediction of bed armoring. Journal of Hydraulic Engineering, 109(4), 611-629. doi:10.1061/(ASCE)0733-9429(1983)109:4(611).

[7] Vázquez-Tarrío, D., Piégay, H., & Menéndez-Duarte, R. (2020). Textural signatures of sediment supply in gravel-bed rivers: Revisiting the armour ratio. Earth-Science Reviews, 207. doi:10.1016/j.earscirev.2020.103211.

[8] Abrahams, A. D., Li, G., Krishnan, C., & Atkinson, J. F. (2001). A sediment transport equation for interrill overland flow on rough surfaces. Earth Surface Processes and Landforms, 26(13), 1443–1459. doi:10.1002/esp.286.

[9] Yang, C. T., & Molinas, A. (1982). Sediment transport and unit stream power function. Journal of the Hydraulics Division, 108(6), 774-793. doi:10.1061/JYCEAJ.0005874.

[10] Zhang, S., Zhu, Z., Peng, J., He, L., & Chen, D. (2021). Laboratory study on the evolution of gravel-bed surfaces in bed armoring processes. Journal of Hydrology, 597. doi:10.1016/j.jhydrol.2020.125751.

[11] Bettess, R., & Frangipane, A. (2003). A one-layer model to predict the time development of static armour. Journal of Hydraulic Research, 41(2), 179–194. doi:10.1080/00221680309499960.

[12] Tait, S. J., Willetts, B. B., & Maizels, J. K. (1992). Laboratory observations of bed armouring and changes in bedload composition. Wiley, New York, United States.

[13] Proffitt, G. T. (1980). Selective transport and armouring of non-uniform alluvial sediments. PhD Thesis, University of Canterbury, Christchurch, New Zealand. Available online: https://ir.canterbury.ac.nz/handle/10092/102035 (accessed on February 2022).

[14] Parker, G., Klingeman, P. C., & McLean, D. G. (1982). Bedload and Size Distribution in Paved Gravel-Bed Streams. Journal of the Hydraulics Division, 108(4), 544–571. doi:10.1061/jyceaj.0005854.

[15] Wilcock, P. R., & Crowe, J. C. (2003). Surface-based transport model for mixed-size sediment. Journal of hydraulic engineering, 129(2), 120-128. doi:10.1061/(ASCE)0733-9429(2003)129:2(120).

[16] Curran, J. C., & Wilcock, P. R. (2005). Effect of Sand Supply on Transport Rates in a Gravel-Bed Channel. Journal of Hydraulic Engineering, 131(11), 961–967. doi:10.1061/(asce)0733-9429(2005)131:11(961).

[17] Wilcock, P. R., & DeTemple, B. T. (2005). Persistence of armor layers in gravel-bed streams. Geophysical Research Letters, 32(8), 1–4. doi:10.1029/2004GL021772.

[18] Bakke, P. D., Basdekas, P. O., Dawdy, D. R., & Klingeman, P. C. (1999). Calibrated Parker-Klingeman Model for Gravel Transport. Journal of Hydraulic Engineering, 125(6), 657–660. doi:10.1061/(asce)0733-9429(1999)125:6(657).

[19] Wilcock, P. R. (2001). Toward a practical method for estimating sediment-transport rates in gravel-bed rivers. Earth Surface Processes and Landforms, 26(13), 1395–1408. doi:10.1002/esp.301.

[20] Tan, L., & Curran, J. C. (2012). Comparison of Turbulent Flows over Clusters of Varying Density. Journal of Hydraulic Engineering, 138(12), 1031–1044. doi:10.1061/(asce)hy.1943-7900.0000635.

[21] Mrokowska, M. M., & Rowinski, P. M. (2019). Impact of unsteady flow events on bedload transport: A review of laboratory experiments. Water (Switzerland), 11(5). doi:10.3390/w11050907.

[22] Berni, C., Perret, E., & Camenen, B. (2018). Characteristic time of sediment transport decrease in static armour formation. Geomorphology, 317, 1–9. doi:10.1016/j.geomorph.2018.04.004.

[23] Elgueta-Astaburuaga, M. A., & Hassan, M. A. (2019). Sediment storage, partial transport, and the evolution of an experimental gravel bed under changing sediment supply regimes. Geomorphology, 330, 1–12. doi:10.1016/j.geomorph.2018.12.018.

[24] Ancey, C. (2020). Bedload transport: a walk between randomness and determinism. Part 2. Challenges and prospects. Journal of Hydraulic Research, 58(1), 18–33. doi:10.1080/00221686.2019.1702595.

[25] Limerinos, J. T. (1969). Determination of the Manning coefficient from measured bed roughness in natural channels. Water Resources Division, Geological Survey, US Department of the Interior, Washington, D.C., United States.

[26] Shields, A. (1936). Application of similarity principles and turbulence research to bed-load movement. Soil Conservation Service, Cooperative Laboratory, California Institute of Technology, Pasadena, United States.

[27] Gomez, B. (2022). The efficiency of the river machine. Geomorphology, 410, 108271. doi:10.1016/j.geomorph.2022.108271.

[28] Wang, Q., Pan, Y., Yang, K., & Nie, R. (2020). Structural properties of the static armor during formation and reestablishment in gravel-bed rivers. Water (Switzerland), 12(7). doi:10.3390/w12071845.

[29] Wang, Q., Li, L., Li, X., Wang, Y., & Nie, R. (2021). Calculation Model to Predict the Static Armor Layer Size Distribution After the Reconstruction of a Gravel River Bed. Frontiers in Earth Science, 9. doi:10.3389/feart.2021.660216.

[30] Anand, A., Beg, M., & Kumar, N. (2021). Experimental studies and analysis on mobilization of the cohesionless sediments through alluvial channel: a review. Civil Engineering Journal, 7(5), 915-936. doi:10.28991/cej-2021-03091700.

[31] van der Meer, J. W. (1986). Deterministic and Probabilistic Design of Breakwater Armour Layers. Dock and Harbour Authority, 67(785), 177–180. doi:10.1061/(asce)0733-950x(1988)114:1(66).

[32] Argente, G., Gómez-Martín, M. E., & Medina, J. R. (2018). Hydraulic stability of the armor layer of overtopped breakwaters. Journal of Marine Science and Engineering, 6(4), 143. doi:10.3390/jmse6040143.

[33] Escarameia, M. (1999). River and channel revetments - a design manual. Thomas Telford, London, United Kingdom. doi:10.1680/racradm.26919.

[34] Eaton, B., & Millar, R. (2017). Predicting gravel bed river response to environmental change: the strengths and limitations of a regime-based approach. Earth Surface Processes and Landforms, 42(6), 994–1008. doi:10.1002/esp.4058.

[35] Ackers, P., & White, W. R. (1973). Sediment Transport: New Approach and Analysis. Journal of the Hydraulics Division, 99(11), 2041–2060. doi:10.1061/jyceaj.0003791.

[36] Płaczkowska, E., Krzemień, K., Gorczyca, E., Bojarczuk, A., & Żelazny, M. (2020). Disturbances in coarse bedload transport in a high-mountain stream channel system (Western Tatras, Poland). Geomorphology, 371, 107428. doi:10.1016/j.geomorph.2020.107428.